Lifetime of the metastable $^2P_{1/2}$ state of F-like Ar^{9+} isolated in a compact Penning trap

Samuel M. Brewer,[1,2,*] Joan M. Dreiling,[1,†] Nicholas D. Guise,[1,2,‡] Shannon F. Hoogerheide,[1]
Aung S. Naing,[3] and Joseph N. Tan[1]

[1]*National Institute of Standards and Technology, 100 Bureau Drive, Gaithersburg, Maryland 20899-8422, USA*
[2]*University of Maryland, College Park, Maryland 20742, USA*
[3]*University of Delaware, Newark, Delaware 19716, USA*

Multiply ionized atoms of a single charge state can be captured at low energy in a compact Penning trap, allowing the measurement of the radiative lifetime of an atomic state that decays via weakly allowed transitions. Such a measurement is reported here for the radiative decay lifetime of the metastable $^2P_{1/2}$ state in fluorinelike Ar^{9+}, wherein the $n = 2$ shell has only one vacancy (hole) in a $2p$ orbital. Highly ionized atoms are extracted from an electron beam ion trap and guided into the ion capture apparatus. Upon capturing the Ar^{9+} ions, light from the magnetic-dipole transition is detected with a photomultiplier tube and counted with a multichannel scaler. Using this technique, the radiative lifetime of the metastable $^2P_{1/2}$ state in Ar^{9+} $1s^2\,2s^2\,2p^5$ is measured to be $\tau = 9.31 \pm 0.08$ ms, consistent with a previous intra-EBIT measurement.

I. INTRODUCTION

Long-lived atomic states are important in many disciplines, including spectroscopic diagnostics of astrophysical or industrial plasmas, fundamental metrology, and tests of basic physics (see [1,2] and references therein). The emission lines of argon ions, for instance, are useful in the analysis of elemental abundances in the solar corona [3]. In metrology, metastable states in neutral or singly ionized atoms are being investigated for developing ultraprecise optical atomic clocks [4]. There is also interest in studying multiply ionized atoms which possess weakly allowed transitions in the optical domain [5,6].

A recently developed method for measuring radiative-decay lifetimes of metastable atomic states involved isolating multiply ionized atoms of interest in a unitary Penning trap [1]. It was shown that lifetime accuracy at the 1% level is feasible by observing the radiative decay of the upper $3d$ fine-structure level of Kr^{17+}—a simple alkali-metal-like ion (K-like). Here, we apply this technique to the more subtle case of Ar^{9+} with an open $2p$ subshell, for which there is some discrepancy in earlier experiments [7–9]. Section II summarizes the ion capture procedure, the optical system for detecting atomic transitions, and some details on the data acquisition. Section III presents the measurement of the radiative lifetime of the metastable $^2P_{1/2}$ state in the $1s^2\,2s^2\,2p^5$ electronic manifold in Ar^{9+}; we compare the new result with predictions and prior measurements.

II. EXPERIMENTAL SETUP

The setup in this work follows [1], apart from upgrades that will be discussed. An electron beam ion trap (EBIT) is used to produce highly charged ions. At NIST, ions can be extracted from the EBIT in bunches. The ion charge state of interest is separated from other charge states using an analyzing magnet and then isolated in a compact Penning trap where the ions are stored at low energy, as described in [10]. The work reported here investigates Ar^{9+} ions, which are created via electron-impact ionization by injecting argon gas into the EBIT. During ion production, the upper fine-structure level $2p^5\,^2P_{1/2}$ is populated by electron-impact excitation. The EBIT is operated with an electron beam energy of 2.5 keV, an electron beam current of 14.7 mA, and ionization time of 20 ms. The highly ionized Ar ions are guided from the EBIT to the Penning trap via electrostatic ion optics in a seven meter long beamline; approximately 500 ions are captured in the Penning trap per bunch [10].

Experiments with the initial setup [1,10] showed the importance of minimizing fluctuations in the trapping conditions. Hence key electronic instruments were upgraded for this work to improve ion capture and storage. In particular, the electrostatic-optic components for ion extraction are now remotely controlled via high-resolution digital-to-analog conversion (DAC) modules to improve stability and reproducibility. Moreover, low-noise high-voltage power supplies are used in operating sensitive components such as the electrodes of the compact Penning trap.

The selected charge state is transferred from the EBIT to the Penning trap with a transit time ($\approx$20.9 μs for Ar^{9+}) that is about 500 times shorter than the radiative decay lifetime of the metastable level. Following charge state selection, the ions are steered further towards the ion capture apparatus with an arrival time spread of $\approx$100 ns. Although the Penning trap was operated under nearly identical conditions as in the earlier measurement for Kr^{17+} [1], the ion production efficiency for Ar^{9+} is higher. After optimizing the setup, the highly ionized Ar ions attain an energy distribution width (full width at half maximum) of about 5.5 eV within 1 ms of capture without any active cooling scheme [10].

———————

*Current address: Time and Frequency Division, NIST, Boulder, CO 80305, USA; samuel.brewer@nist.gov

†Current address: Honeywell, Broomfield, CO 80021, USA.

‡Current address: Quantum Systems Division, Georgia Tech Research Institute, Atlanta, GA 30332, USA.
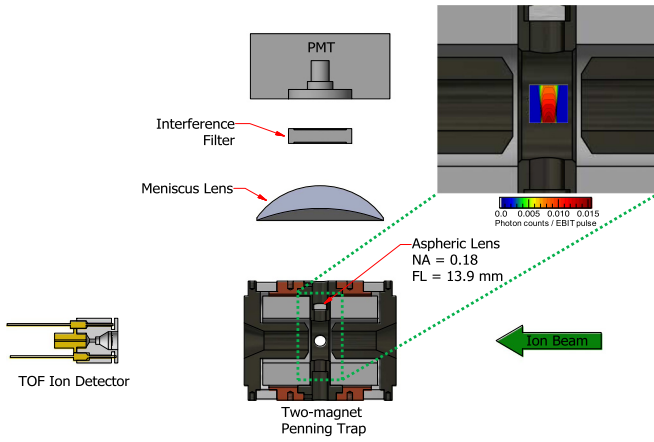
FIG. 1. Schematic diagram for the detection of radiative decay from ions captured in a unitary Penning trap. Ion bunches are periodically injected into the trap to build up statistics. A small aspheric lens in the ring electrode collects photons emitted by stored ions. A set of lenses and a filter centered at 550 nm allows a 40 nm band of light to be relayed to a photon detector. After each measurement cycle, the trapped ions are counted by ejection to a time-of-flight (TOF) detector. (Inset) Optical transfer function simulation for the absolute number of detected photons per data acquisition cycle. The calculations are performed in a coordinate system which is aligned with the optical axis.

FIG. 2. Measured radiative decay lifetime of the $^2P_{1/2}$ state of Ar^{9+} for a base pressure of 8.0×10^{-8} Pa. Top: observed photon counts (black) as a function of time after ion capture along with a fit (red) described by Eq. (1). Bottom: deviations from the best-fit function, plotting normalized residuals (Δ_i/σ_Δ), where Δ_i is the difference between the exponential fit result $N(t_i)$ and the measured photon data N_i and σ_Δ is the global standard deviation of the residuals. For this data set $\chi^2/\nu = 1.05$.

III. LIFETIME OF THE $^2P_{1/2}$ STATE IN Ar^{9+}

A. Measurement

A representative radiative decay curve at the lowest ambient (base) pressure (P = 8.0×10^{-8} Pa) is shown in Fig. 2. The measured decay data has been fit to a single exponential
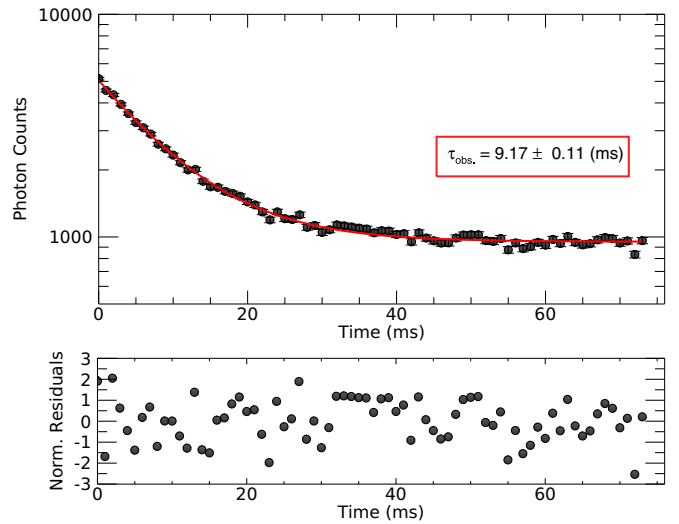
Figure 1 shows a schematic diagram of the optical setup used to measure the lifetimes of metastable states of ions isolated in the unitary Penning trap. As the metastable atomic state decays, photons emitted by stored ions are collected by an aspheric lens embedded in the ring electrode at the midplane of the trap. Outside the ion trap vacuum enclosure, a lens system relays the collected photons to a commercial photon-counting system (Hamamatsu H7421-40) [11]. The detector is a GaAsP photocathode operated in Geiger mode for photon counting in the wavelength range from 300 nm to 720 nm, with a peak quantum efficiency of 40% at 580 nm. When this photomultiplier (PMT) is cooled to $-20\,^\circ$C and electrical noise is minimized, the average dark count rate can be as low as $3\,\mathrm{s}^{-1}$. Stray light is minimized by using an interference filter with a 40 nm bandpass centered near the wavelength of interest $\lambda = 553.3265(2)$ nm for Ar^{9+} [12]. The measurement cycle begins with the arrival of the ion bunch in the Penning trap; simultaneous with the closing of the trapping potential well, a multichannel scaler (MCS) is triggered to begin counting photons in 1 ms time bins for a specified duration (capture and storage cycle) of up to 74 ms. At the end of each such MCS measurement cycle, ions are ejected from the Penning trap and counted on a time-of-flight (TOF) detector. The measurement cycle is then repeated with a new bunch of ions.

function given by

$$N(t) = N_o e^{-t/\tau_{obs}} + B, \tag{1}$$

where N_o is the number of detected photons at $t = 0$, τ_{obs} is the radiative decay constant of interest, and B is the integrated background level due to dark counts. At base pressure, the radiative decay constant is measured to be $\tau_{obs} = 9.17 \pm 0.11$ ms. A decay rate is obtained by taking the reciprocal of the lifetime

$$\gamma_{obs} = \frac{1}{\tau_{obs}}, \tag{2}$$

yielding $\gamma_{obs} = 109.03 \pm 1.30_{stat}$ s^{-1}. The fitted background $B = 951.8 \pm 5.3$ counts/time bin is consistent with the average dark count rate integrated for $\approx 200\,000$ measurement cycles.

In this work, photon counting statistics account for the largest uncertainty, but small systematic corrections also add to the overall uncertainty. The corrections and associated uncertainties are summarized in Table I. Systematic effects that depend on the background gas density, such as charge exchange, can be minimized by extrapolation of measurements at various vacuum pressures (P), as illustrated in a Stern-Volmer plot (Fig. 3) for Ar^{9+}. The P $\rightarrow$ 0 extrapolated lifetime is $\tau_{P \rightarrow 0} = 9.36 \pm 0.08$ ms.

An additional correction comes from the fact that the ion loss rate typically does not extrapolate to zero in the ideal vacuum limit. This correction addresses the ion cloud expansion in the presence of instabilities driven by trap imperfections. The ion storage times are also measured at various background gas pressures and extrapolated to the P $\rightarrow$ 0 limit giving an estimated +0.030(3) ms correction to the radiative lifetime.

TABLE I. Corrections and sources of statistical and systematic uncertainty.

Effect	Shift (ms)	Uncertainty (ms)
Photon counting statistics	0.0	0.080
Measured ion cloud expansion	0.0	0.003
Total statistical uncertainty	0.0	0.080
Ion-beam alignment	0.0	(−0.000,+0.050)
Ion-loss correction	0.016	(−0.000,+0.016)
Pressure gauge offset	0.0	0.014
Interference filter orientation	0.0	0.010
Modeling of optics and ion motions	0.0	0.010
Axial ion loss	0.0	0.001
Cascade repopulation	0.0	0.001
Reexcitation by cold-electron impact	0.0	0.001
Total systematic shift and uncertainty	0.016	(−0.02, +0.06)

TABLE II. Calculations of the lifetime τ of the $^2P_{1/2}$ level in Ar^{9+}. The column $\Delta\lambda$ gives the difference $\Delta\lambda = \lambda_{th} - \lambda_{exp}$ between the calculated wavelength λ_{th} and the observed wavelength λ_{exp}.

Year	Method	λ_{th} (nm)	$\Delta\lambda$ (nm)	τ (ms)	τ_{adj} (ms)
1966	HFSCF[a] [15]	553.60	+0.27	9.52	9.51
1979	MCDF[b] [16]	556.00	+2.67	9.58	9.44
1986	MCDF [17]	553.34	+0.01	9.43	9.43
2004	MCHF+BP[c] [18]	549.68	−3.65	9.24	9.42
2013	MCDHF[d] [19]	553.53	+0.20	9.44	9.43
2016	RCC+BP[e] [20]	554.10	+0.77	9.34	9.30
2018	MCDHF[d] [21]	553.48	+0.15	9.40	9.39

[a]Hartree-Fock self-consistent field.
[b]Multiconfiguration Dirac-Fock.
[c]Multiconfiguration Hartree-Fock plus Breit-Pauli.
[d]Multiconfiguration Dirac Hartree-Fock.
[e]Relativistic coupled-cluster plus Breit-Pauli.

However, this technique tends to overestimate the ion-loss correction to the radiative lifetime due to, e.g., ions that remain in the effective field of view of the PMT even when they are no longer detectable in the TOF signal. In a Penning trap, the well-characterized motions of the trapped ions allow for a detailed analysis of systematic corrections. In particular, we can compute more precisely the appropriate ion-loss correction by accounting for those ions discussed above that are detectable by the PMT but not the TOF. This involves a non-neutral plasma simulation of the ion cloud dimensions [13] and an extensive tracing of light paths to the PMT. The ion cloud model is constrained by the observed TOF signal as described in [14]. As listed in Table I, this refined ion-loss correction to the $M1$ lifetime is +0.016(3) ms.

The dominant systematic uncertainty is due to residual ion-beam misalignment during capture. We found a weak dependence of the radiative decay lifetime on the electrostatic tuning for injection of selected ions into the Penning trap. As discussed in [10], off-axis ion injection into the Penning trap tends to broaden the spatial distribution of captured ions and raise
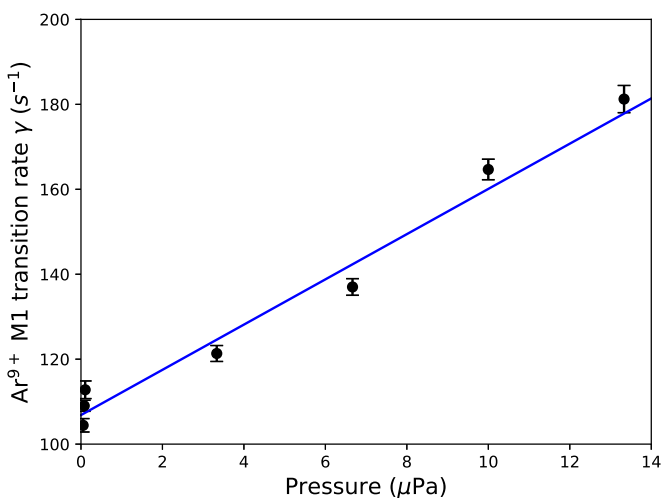

FIG. 3. Stern-Volmer analysis of the $^2P_{1/2}$ radiative decay rate in Ar^{9+}. An extrapolation of the measured decay rate as P → 0 approaches the ideal vacuum limit.

the temperature. This tends to shorten the observed radiative lifetime slightly. The effect was investigated by deliberately mistuning the voltages on the electrodes that steer the extracted ions into the Penning trap. During data acquisition, the ion TOF signal was monitored routinely after 1 ms of storage to account for any long-term beam steering drifts. Given the improvement in beam steering reproducibility, trapped ion number, and ion storage lifetime, we assign (−0.00, +0.05) ms for the systematic uncertainty due to possible ion-beam misalignment.

Other minor sources of uncertainty include a possible offset in the pressure gauge readings, which is estimated using the maximum offset consistent with a positive ion cloud expansion rate [14]. Finally, the transmission efficiency of the interference filter (40 nm passband) depends on the relative angle of the light path, contributing an uncertainty of 0.01 ms.

In brief, the leading uncertainties come from photon counting statistics and a sensitivity to the ion-beam misalignment during the ion capture process. With the corrections to the P → 0 lifetime listed in Table I, we obtain

$$\tau = 9.38 \,(\pm 0.08)_{stat} \binom{+0.06}{-0.02}_{syst} \text{ ms} \qquad (3)$$

for the radiative lifetime of the $2p^5\ {}^2P_{1/2}$ level in Ar^{9+}.

B. Discussion of results

Theoretical efforts since 1966 have yielded seven predictions for the lifetime of the $1s^22s^22p^5\ {}^2P_{1/2}$ level in Ar^{9+}; they are listed in Table II and plotted in Fig. 4 as yellow-filled triangles. The average *ab initio* prediction is 9.43 ms, with a sample spread (standard deviation) of 0.10 ms.

The magnetic-dipole transition that is mainly responsible for the radiative decay of the $^2P_{1/2}$ to the $^2P_{3/2}$ ground state in Ar^{9+} has a strong dependence on the wavelength of the emitted light. Column 4 of Table II shows that the calculated wavelength can differ by more than 3 nm between methods. The most precise value for the observed wavelength was reported in 2003 to be $\lambda_{exp} = 553.3265(2)$ nm, consistent with an earlier measurement (1969) that is two orders of magnitude less precise [12]. Errors due to the cubic dependence of the calculated lifetime on the transition wavelength can
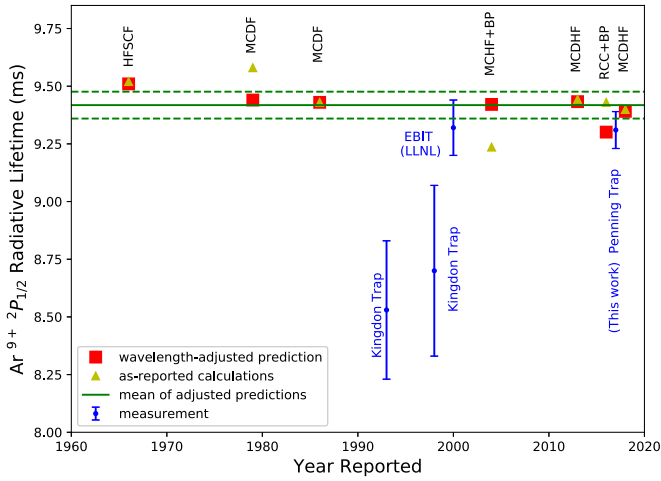
FIG. 4. Comparison of calculations and measurements of the radiative decay lifetime of the Ar^{9+} $^2P_{1/2}$ level. Yellow-filled triangles represent calculated values as reported; red-filled squares correspond to wavelength-adjusted results. The error bars of each measurement (blue circle) indicate one standard error. The average of the adjusted theoretical lifetime calculations is shown in the solid green line, with the standard deviation of the predictions denoted by the green dashed lines.

be removed by rescaling; we report the adjusted values τ_{adj} in the last column of Table II, plotting them as red-filled squares in Fig. 4. The average of adjusted lifetime values is 9.42 ms, plotted as a green solid line in Fig. 4. By using the observed wavelength, the scatter of the wavelength-adjusted values is reduced by a factor of 5/3 to a standard deviation of 0.06 ms, as depicted by the two green dashed lines.

For comparison, Fig. 4 shows the four measurements of the radiative decay lifetime of the Ar^{9+} $^2P_{1/2}$ level and the results are also listed in Table III. The earliest experiments employed an electron cyclotron resonance ion source (ECRIS) to produce and extract multiply charged ions that were then captured in a Kingdon-type electrostatic ion trap. In those measurements, the extracted Ar^{9+} ions were injected into the midplane of the Kingdon trap via symmetrical apertures in the wall of its cylindrical electrode. The first Kingdon trap experiment gave a lifetime value of 8.53(30) ms [7], which disagrees with theory by about three standard deviations. The second measurement with a Kingdon trap yielded a lifetime of 8.70(37) ms [8], which

TABLE III. Measurements of the radiative decay lifetime of the metastable $^2P_{1/2}$ state in Ar^{9+}. The ion trapping device used during photon counting is indicated under "Trap type."

Year	Lifetime (ms)	Ion source	Trap type
1994	8.53 ± 0.30	ECRIS[a]	Kingdon[b] [7]
1998	8.70 ± 0.37	ECRIS	Kingdon [8]
2000	9.32 ± 0.12	EBIT (LLNL)	EBIT[c] [9]
2017	9.31 ± 0.08	EBIT (NIST)	Penning

[a]Electron cyclotron resonance ion source.

[b]Electrostatic Kingdon trap.

[c]Magnetic trapping mode with electron beam switched off.

is consistent with the first measurement, but disagrees with theory by two standard deviations. These two Kingdon trap experiments can be combined to give a weighted mean $\tau_{KT} = 8.60 \pm 0.23$ ms, which has a 3.6σ (uncertainties combined in quadrature) discrepancy with theory.

The third experiment was undertaken at Lawrence Livermore National Laboratory (LLNL) using a cryogenic EBIT operated in the magnetic trapping mode [9]. The measurement made inside the LLNL EBIT gave a lifetime of $\tau_{LLNL} = 9.32 \pm 0.12$ ms, which is higher than the Kingdon trap result by $2.8\sigma_{combined}$. The LLNL EBIT result agrees well with some predictions and is lower than the mean of adjusted predictions by less than 1σ.

In the latest measurements with Ar^{9+} ions isolated in a unitary Penning trap, we obtained a $^2P_{1/2}$ lifetime of $\tau = 9.38 \pm 0.08_{stat}(-0.02, +0.06)_{syst}$ ms. Combining all statistical and systematic uncertainties in quadrature gives a total uncertainty of $(-0.084, +0.098)$ ms. Since the asymmetry in the error bars is not significant, we simplify the result with the symmetrized form: $\tau = 9.38 \pm 0.09$ ms.

A previous measurement using this apparatus, prior to the upgrade in electronic equipment necessary for better trapping stability, yielded a lifetime of $\tau = 8.9 \pm 0.2$ ms [22] following similar systematic analysis as presented here, but with larger statistical uncertainty. Combining all available data from this apparatus, we arrive at a final radiative lifetime of $\tau = 9.31 \pm 0.08$ ms. As illustrated in Fig. 4, the compact Penning trap result agrees well with the LLNL EBIT measurement and is $1.1\sigma_{combined}$ lower than the mean of the wavelength-adjusted predictions (green line).

IV. SUMMARY

Multiple charge states of argon are extracted in bunches from the EBIT at NIST. Fluorinelike Ar^{9+} ions are selected by an analyzing magnet, and the ions are then guided to a unitary Penning trap. Here, the selected charge state is captured and stored for light collection to measure the radiative lifetime of the $^2P_{1/2}$ metastable state. This method yields a lifetime $\tau = 9.31 \pm 0.08$ ms for the $^2P_{1/2}$ level, the upper fine-structure level of the electronic ground configuration. This measurement is consistent with the earlier result from an intra-EBIT experiment [9] which had different systematic effects.

The final uncertainty of 1% in this work is smaller than achieved in earlier measurements. This improvement was attained mainly from apparatus upgrades that increased the stability and reproducibility of ion capture conditions. Higher precision seems possible if the compact Penning trap is redesigned to enhance light collection efficiency. A factor of 10 improvement in accuracy would be necessary to test theoretical calculations that include contributions from quantum electrodynamics (QED) [23]. In addition, the electric quadrupole ($E2$) decay rate is of interest as a test of QED [9,21]. The $E2$ decay rate is expected to be much weaker than the $M1$ rate [9,21], making it a challenge to observe using the current experimental setup. To facilitate such investigations, a miniature EBIT ion source is being developed to enable continual operation without incurring the cost of a high magnetic-field EBIT that requires cryogens [24,25].

[1] N. D. Guise, J. N. Tan, S. M. Brewer, C. F. Fischer, and P. Jönsson, Phys. Rev. A **89**, 040502(R) (2014).

[2] S. F. Hoogerheide, A. S. Naing, J. M. Dreiling, S. M. Brewer, N. D. Guise, and J. N. Tan, Atoms **3**, 367 (2015).

[3] P. R. Young, H. E. Mason, F. P. Keenan, and K. G. Widing, Astron. Astrophys. **323**, 243 (1997).

[4] A. D. Ludlow, M. M. Boyd, J. Ye, E. Peik, and P. O. Schmidt, Rev. Mod. Phys. **87**, 637 (2015).

[5] A. Windberger, J. R. Crespo López-Urrutia, H. Bekker, N. S. Oreshkina, J. C. Berengut, V. Bock, A. Borschevsky, V. A. Dzuba, E. Eliav, Z. Harman, U. Kaldor, S. Kaul, U. I. Safronova, V. V. Flambaum, C. H. Keitel, P. O. Schmidt, J. Ullrich, and O. O. Versolato, Phys. Rev. Lett. **114**, 150801 (2015).

[6] M. S. Safronova, V. A. Dzuba, V. V. Flambaum, U. I. Safronova, S. G. Porsev, and M. G. Kozlov, Phys. Rev. Lett. **113**, 030801 (2014).

[7] L. Yang, D. A. Church, S. Tu, and J. Jin, Phys. Rev. A **50**, 177 (1994).

[8] D. P. Moehs and D. A. Church, Phys. Rev. A **58**, 1111 (1998).

[9] E. Träbert, P. Beiersdorfer, S. B. Utter, G. V. Brown, H. Chen, C. L. Harris, P. A. Neill, D. W. Savin, and A. J. Smith, Astrophys. J. **541**, 506 (2000).

[10] S. M. Brewer, N. D. Guise, and J. N. Tan, Phys. Rev. A **88**, 063403 (2013).

[11] Identification of a product herein is for documentation purposes only; no recommendation or endorsement by NIST is implied.

[12] I. Draganić, J. R. Crespo López-Urrutia, R. DuBois, S. Fritzsche, V. M. Shabaev, R. S. Orts, I. I. Tupitsyn, Y. Zou, and J. Ullrich, Phys. Rev. Lett. **91**, 183001 (2003).

[13] R. L. Spencer, S. N. Rasband, and R. R. Vanfleet, Phys. Fluids B **5**, 4267 (1993).

[14] S. M. Brewer, Ph.D. thesis, University of Maryland at College Park, 2012.

[15] T. K. Krueger and S. J. Czyzak, Astrophys. J. **144**, 1194 (1966).

[16] K. Cheng, Y. Kim, and J. Desclaux, At. Data Nucl. Data Tables **24**, 111 (1979).

[17] V. Kaufman and J. Sugar, J. Phys. Chem. Ref. Data **15**, 321 (1986).

[18] C. F. Fischer and G. Tachiev, At. Data Nucl. Data Tables **87**, 1 (2004).

[19] P. Jönsson, A. Alkauskas, and G. Gaigalas, At. Data Nucl. Data Tables **99**, 431 (2013).

[20] D. K. Nandy, Phys. Rev. A **94**, 052507 (2016).

[21] M. Bilal, A. V. Volotka, R. Beerwerth, and S. Fritzsche, Phys. Rev. A **97**, 052506 (2018).

[22] S. M. Brewer, N. D. Guise, S. F. Hoogerheide, and J. N. Tan (private communication).

[23] A. Lapierre, U. D. Jentschura, J. R. Crespo López-Urrutia, J. Braun, G. Brenner, H. Bruhns, D. Fischer, A. J. González Martínez, Z. Harman, W. R. Johnson, C. H. Keitel, V. Mironov, C. J. Osborne, G. Sikler, R. Soria Orts, V. Shabaev, H. Tawara, I. I. Tupitsyn, J. Ullrich, and A. Volotka, Phys. Rev. Lett. **95**, 183001 (2005).

[24] S. Hoogerheide and J. Tan, J. Phys.: Conf. Ser. **583**, 012044 (2015).

[25] A. Naing, S. Hoogerheide, J. Dreiling, and J. Tan, http://meetings.aps.org/link/BAPS.2016.DAMOP.Q1.23